Vertical Federated Learning Across Second-hop Parties

Abstract. Vertical federated learning (VFL) enables parties with different features to collaboratively develop models on overlapping samples without directly sharing raw data. Conventional VFL systems typically require data overlap among all parties to perform training and inference. Recent work has relaxed this assumption to allow federated inference on non-overlapping samples. However, current methods struggle to handle scenarios where the active party only shares sample overlap with a subset of passive parties, thereby missing critical feature information from non-overlapping parties. We introduce *Vertical Federated Learning Across Second-hop Parties* (VFL-ASP), an enhanced VFL framework that improves feature utilization across second-hop passive parties. These parties have overlapping data with first-hop passive parties, which in turn share overlap with the active party. VFL-ASP extracts hidden embeddings from overlapping samples among second-hop and first-hop parties under encrypted federation and learns embedding approximations, which are then utilized alongside the active party data for training and inference. We apply knowledge distillation to refine a student model with soft labels from the VFL teacher model, enabling local processing of non-overlapping data. Our evaluation of three real-world datasets demonstrates that VFL-ASP achieves improved performance accuracy over traditional VFL baselines.

Keywords: vertical federated learning · second-hop parties · embedding extraction

1 Introduction

Federated learning (FL) provides a decentralized method to train a machine learning model over distributed data without explicitly sharing data across local parties, thereby providing privacy and security benefits [13–15, 17, 21, 28]. Federated learning has been extensively used in many domains, particularly in healthcare, where collaboration across hospitals enables global hypothesis testing and subgroup analyses, surpassing the localized hospital settings. [4]. Vertical federated learning (VFL) uses vertically partitioned data, where multiple parties with distinct features over the same samples jointly train machine learning models without sharing their raw data or model parameters. Each party trains a local model and uploads intermediate results to the global model as input for training. The global model then sends the gradients back to each local model for parameter updates, and all parties conduct inference collaboratively [19]. VFL

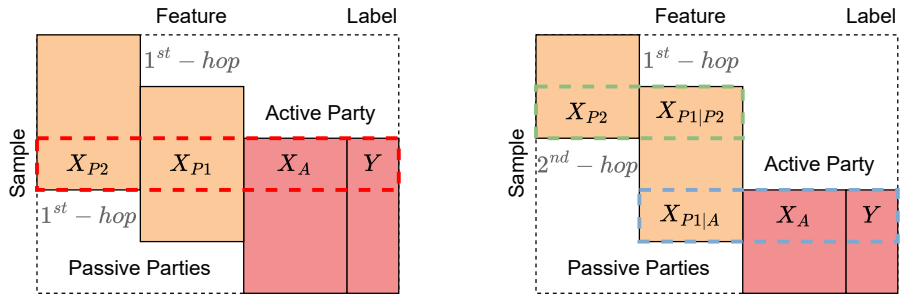

(a) Standard data distribution assumes data overlap among all parties.

(b) No data overlap exists between the second-hop passive and active parties.

Fig. 1: VFL data overlap configurations.

has emerged as a promising paradigm for privacy-preserving inference in settings with shared data samples but distinct features [26].

Standard VFL systems assume multiple passive parties contribute features, while the active party provides both features and labels. In addition, only overlapping data shared across all (passive and active) parties is used for training local and global models, as well as for inference. Figure 1a shows such a shared data overlap (the dotted red box) between passive parties $P1, P2$ (denoted in orange), and active party A (denoted in red).

Unfortunately, the assumption that all passive parties share common data overlap with the active party rarely holds in practice due to data-sharing constraints, heterogeneous data sources, and other factors. Different data usage policies across parties lead to varying features. Existing work has provided solutions to allow inference on local, non-overlapping data while still requiring overlapping data from all parties for training [10, 16, 23]. These methods are unable to leverage critical feature information from (the second-hop) passive parties that do not directly overlap with the active party, but share overlap with intermediate (the first-hop) parties that overlap with the active party. Figure 1b shows such an example setting where the second-hop passive party $P2$ does not directly overlap with the active party but is connected through the first-hop, intermediate passive party (the dotted green box), who in turn, overlaps with the active party (the dotted blue box). Such data overlap configurations pose challenges in traditional VFL methods, as highlighted in the following example.

Example 1. Figure 2 illustrates a clinical hospital data configuration where Hospital A (the active party) contains patient demographic information as the feature and disease outcomes as the label. Hospital $P1$ (the first-hop passive party) holds patient lab results, and shares overlapping data with both Hospital A (via blue records) and Hospital $P2$ (via green records). Hospital $P2$ (the second-hop passive party) stores the data feature on previous treatments, which is critical for predicting disease outcomes, but only shares overlapping records with Hospital $P1$.

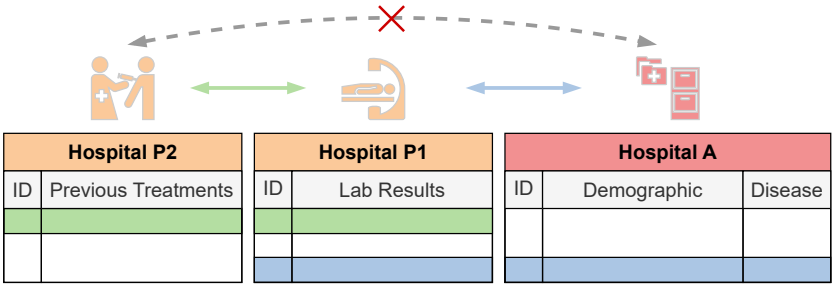

Fig. 2: Healthcare example with three hospitals.

We introduce Vertical Federated Learning Across Second-hop Parties (VFL-ASP), a novel framework that incorporates features from the second-hop parties during learning and inference. VFL-ASP first extracts hidden embeddings under encrypted federation from overlapping data between the first and second-hop parties, and then utilizes auto-encoder to perform semi-supervised learning to generate embedding approximations that capture feature information learned from the second-hop parties. Subsequently, the framework leverages these approximations (instead of local data from first-hop) alongside active party data to construct a VFL system. To enhance the capability, VFL-ASP employs knowledge distillation, enabling a student model at the active local party to make inferences independently, supervised by the VFL teacher model.

We propose a more efficient approach to federated Singular Value Decomposition (SVD) by concatenating encrypted overlapping data from the first-hop and second-hop parties, enabling hidden embedding extraction with a single encryption matrix. We formally demonstrate the proof of our approach. In contrast, previous approaches are designed to use the summation of overlapping data with two encryption matrices (left and right orthogonal masks), leading to higher computation costs [2, 10].

We evaluate our model on three real-world datasets with diverse data partitioning strategies to explore varying feature splits and sample overlaps among parties, comparing its performance against standard VFL and local models. The results show that VFL-ASP consistently achieves the highest accuracy, particularly outperforming standard VFL and local model by $+1.387\%$ and $+5.474\%$ accuracy, respectively. We perform an ablation study to assess the effectiveness of the extracted embeddings and conduct a runtime analysis to evaluate efficiency.

Contributions. We make the following contributions:

1. We introduce VFL-ASP, a new framework that integrates feature information from the second-hop passive parties into the training and inference process.
2. We propose a more efficient usage of federated SVD via the concatenation of encrypted overlapping data from the first-hop and second-hop parties to extract hidden embeddings with a single encryption matrix.
3. We evaluate our model on three real-world datasets with varying feature splits and sample overlaps among parties. Our evaluation also includes an ablation study and runtime analysis.

2 Overview

We provide a brief introduction of VFL and then describe the architecture of VFL-ASP. The notations used in this study are given in Table 1.

Table 1: Notation summary.

Symbol	Description
$X_i, X_{i\|j}$	Data matrices of party i and i overlapped with j
X_i^e	Encrypted data for federated SVD
G, M_i	Global and local models
ϕ, θ_i	Global and local parameters
Y	Ground truth label
$\hat{Y}, \tilde{Y}$	Model prediction and soft label
$E, \hat{E}$	Decrypted embedding and embedding approximation

2.1 Vertical Federated Learning

Define X_i^{Sample} and $X_i^{Feature}$ as the sample and feature space corresponding to the matrix's rows and columns, respectively. Without loss of generality, consider two passive parties, $P1$ and $P2$, and an active party A. The necessary conditions for VFL are: $X_{P2}^{Feature} \neq X_{P1}^{Feature} \neq X_A^{Feature}$, ensuring unique features for each party, and $X_{P2}^{Sample} = X_{P1}^{Sample} = X_A^{Sample}$, indicating a common shared sample overlap among all parties.

Suppose the collaborative training is based on the overlapping data with m samples among k parties and each party holds n_i features. Then, each party owns a data source $X_i \in \mathbb{R}^{m \times n_i}$. Hence the problem can be formulated as:

$$\min \mathcal{L}_{vfl}(G(_{\phi|M_1(\theta_1|X_1),\ldots,M_k(\theta_k|X_k)}), Y),$$

where the VFL training loss $\mathcal{L}_{vfl}$ is computed from the global model G with ground truth Y.

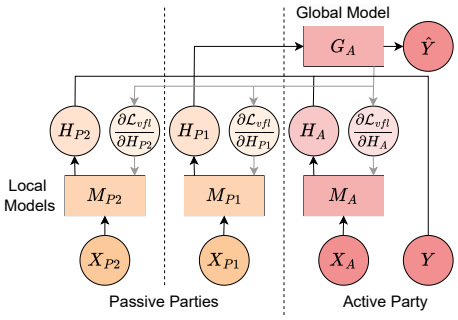

Fig. 3: VFL training procedure.

Training Procedure. The training procedure is shown in Figure 3. Passive parties typically only communicate with the active party, which acts as the coordinator to control the training and inference process of the global model.

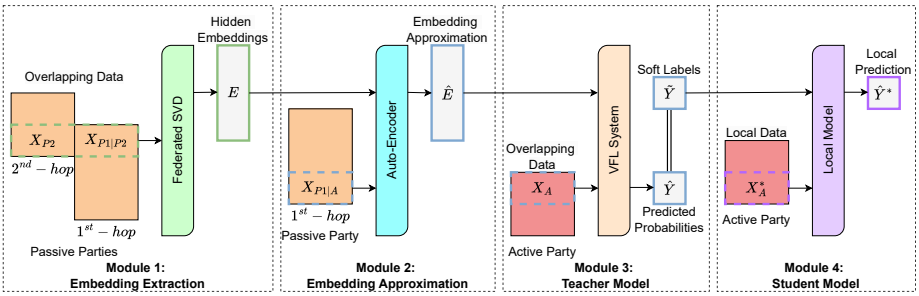

Fig. 4: Framework overview of VFL-ASP.

However, in certain scenarios, a third party may be involved, responsible for encryption and decryption tasks [20]. Each party will train a local model M_i with its private data X_i first and then send the intermediate outputs H_i to the active party without directly sharing raw data. Next, the active party will feed these intermediate results into a global model G with ground truth Y to compute the training loss $\mathcal{L}_{vfl}$ for updating the global parameters ϕ by the partial derivative $\frac{\partial \mathcal{L}_{vfl}}{\partial \phi}$. Then, the active party will send gradients $\frac{\partial \mathcal{L}_{vfl}}{\partial H_i}$ back to each local model. Finally, the local models will update the local parameters θ_i until convergence by the following chain rule for the partial derivative:

$$\frac{\partial \mathcal{L}_{vfl}}{\partial \theta_i} = \frac{\partial \mathcal{L}_{vfl}}{\partial H_i} \frac{\partial H_i}{\partial \theta_i}.$$

During inference with new data samples, each party will first generate the intermediate outputs with unique feature information and then the global model will utilize these intermediate results to generate the prediction $\hat{Y}$.

Privacy and Security. In a standard VFL system, privacy risks can arise inside and outside. Inside refers to privacy risks that arise from within the system itself. Outside refers to privacy risks originating from external entities such as external attackers. The parties within the system can be labeled as honest, semi-honest, or malicious. A semi-honest attacker obeys the VFL protocol but seeks to access the private data of other parties, whereas a malicious attacker violates the VFL protocol. Privacy-preserving protocols involved in a typical VFL framework are extensively covered in the survey [19]. In this study, we assume all parties are semi-honest, which is widely accepted in the FL system [26]. Although weaker than the malicious setting, this assumption is highly efficient. Under this setting, all parties strictly adhere to the protocol, yet they may be curious about other parties and attempt to obtain additional information from the transferred data.

2.2 VFL-ASP Architecture

The architecture of VFL-ASP is illustrated in Figure 4, which proceeds along four main modules. We develop the initial two modules as extensions for VFL systems to leverage feature information from the second-hop passive parties, ensuring easy integration with the existing VFL frameworks.

Embedding Extraction: We first extract hidden embeddings under encrypted federation from shared overlapping data using federated SVD.
Embedding Approximation: We apply semi-supervised training using an auto-encoder to approximate the embeddings. By utilizing the first two modules, VFL-ASP enables the integration of features from second-hop passive parties.
Teacher (VFL) Model: The framework leverages the approximations (instead of local data from first-hop) alongside active party data to construct a VFL system, generating both predictions and soft labels.
Student Model: The soft labels reflect the probability distribution of VFL predictions, which supervise a student model on the local active party to allow inference independently.

3 Methodology

3.1 Embedding Extraction

Federated SVD. We propose an efficient approach to federated Singular Value Decomposition (SVD) to extract hidden embeddings E from overlapping data X_{P2} and $X_{P1|P2}$, inspired by FedSVD [2]. Original FedSVD aims to achieve lossless accuracy and high efficiency without directly sharing raw data by using matrix masking technique. For a given matrix $X \in \mathbb{R}^{m \times n}$, SVD decomposes it into three matrices:

$$X = U \Sigma V^T,$$

where $U \in \mathbb{R}^{m \times m}$ and $V^T \in \mathbb{R}^{n \times n}$ are orthogonal matrices containing left and right singular vectors, and $\Sigma \in \mathbb{R}^{m \times n}$ is a diagonal matrix with singular values in decreasing order. In a typical federated SVD scenario with k parties, each possessing a data matrix $X_i \in \mathbb{R}^{m \times n_i}$, where m represents the number of overlapping samples, n_i is the number of features within each party, and $\sum_{i=1}^{k} n_i = n$. These k parties collectively perform SVD on the concatenated data $[X_1, ..., X_k] = X \in \mathbb{R}^{m \times n}$, yielding:

$$[X_1, ..., X_k] = U \Sigma [V_1^T, ..., V_k^T].$$

Each party derives the result as $X_i = U \Sigma V_i^T$, where $U \in \mathbb{R}^{m \times m}$ and $\Sigma \in \mathbb{R}^{m \times n}$ are shared among all parties, but $V_i^T \in \mathbb{R}^{n \times n_i}$ can only be accessed by party i.

The FedSVD framework implements federated SVD by encrypting the private data by multiplying two random orthogonal matrices on both sides at the beginning, which can be fully removed from the SVD results in the end [2]. While FedSVD discusses both orthogonal matrices U and V in detail, for brevity, we will discuss U only. Assuming k parties are sharing overlapping samples, the overlapping data can be represented as $X = [X_1, ..., X_k]$. To ensure privacy preservation, a trusted third party generates two random orthogonal matrices $P \in \mathbb{R}^{m \times m}$ and $Q^T \in \mathbb{R}^{n \times n}$. Q^T is further split into k matrices $Q^T = [Q_1^T, ..., Q_k^T]$, where $Q_i^T \in \mathbb{R}^{n \times n_i}$. The third party sends P and Q_i^T to each party, which then sends

the encrypted data $X_i^\epsilon = PX_iQ_i \in \mathbb{R}^{m\times n}$ to a semi-honest central server. Since we know that

$$PXQ = P[X_1, ..., X_k][Q_1^T, ..., Q_k^T]^T = \sum_{i=1}^{k} PX_iQ_i = \sum_{i=1}^{k} X_i^\epsilon,$$

we can set $PXQ = X^\epsilon$. Therefore, $\sum_{i=1}^{k} X_i^\epsilon = X^\epsilon$. The server then runs the SVD algorithm on the summation of the encrypted data from k parties, resulting in $X^\epsilon = U^\epsilon \Sigma^\epsilon V^{\epsilon T}$. Thus, we obtain

$$X = P^T X^\epsilon Q^T = P^T U^\epsilon \Sigma^\epsilon V^{\epsilon T} Q^T.$$

If we run the SVD algorithm on raw data X directly, we get $X = U\Sigma V^T$. Since orthogonal matrices only represent rotations and reflections, and do not change the magnitude of vectors, the singular values represented by Σ and Σ^ϵ are equal. Therefore, $\Sigma = \Sigma^\epsilon$ and

$$[P^T U^\epsilon]\Sigma^\epsilon[V^{\epsilon T} Q^T] = U\Sigma^\epsilon V^T.$$

We may use $P^T U^\epsilon$ to approximate U [2]. Lastly, the server releases the encrypted orthogonal matrix U^ϵ to the k parties, and each party uses $P^T U^\epsilon$ to approximate U.

Hidden Embeddings. VFL-ASP utilizes a single random orthogonal matrix $P \in \mathbb{R}^{m\times m}$, generated by a trusted third party and distributed to each passive party. Each party then encrypts its data as $X_i^\epsilon = PX_i \in \mathbb{R}^{m\times n_i}$ and sends it to a semi-honest central server (operated by the active party). Given that

$$PX = P[X_1, ..., X_k] = [PX_1, ..., PX_k] = [X_1^\epsilon, ..., X_k^\epsilon],$$

we can set $PX = X^\epsilon \in \mathbb{R}^{m\times n}$. The server runs the SVD algorithm on the concatenation of the encrypted data matrices instead of their summation, resulting in $X^\epsilon = U^\epsilon \Sigma^\epsilon V^{\epsilon T}$. Thus, we have

$$X = P^T X^\epsilon = P^T U^\epsilon \Sigma^\epsilon V^{\epsilon T}.$$

Similarly, since the SVD result of raw data X is $X = U\Sigma V^T$ and $\Sigma^\epsilon = \Sigma$, then we get

$$[P^T U^\epsilon]\Sigma^\epsilon V^{\epsilon T} = U\Sigma^\epsilon V^T.$$

Finally, the server releases the encrypted orthogonal matrix U^ϵ and singular value Σ^ϵ back to the k parties. Each party can approximate U with $P^T U^\epsilon$ and approximate $U\Sigma$ using $[P^T U^\epsilon]\Sigma^\epsilon$, which is the decrypted hidden embedding E we want to extract.

Note that directly recovering X from X^ϵ without knowing P is not possible, even if the server knows the SVD result of X^ϵ. This guarantees data privacy between the passive parties and the active party. In practical scenarios where $m \gg n$, to reduce computational costs, we trim the encrypted orthogonal matrix U^ϵ from $\mathbb{R}^{m\times m}$ to $\mathbb{R}^{m\times n}$, preserving only the first n significant columns. Σ^ϵ keeps the singular values and forms a diagonal matrix as $\mathbb{R}^{n\times n}$. Eventually, the first-hop passive party obtains the decrypted embedding matrix E as $[P^T U^\epsilon]\Sigma^\epsilon \in \mathbb{R}^{m\times n}$, which shares the same dimensions as the original overlapping data X.

3.2 Embedding Approximation

We employ a standard autoencoder architecture, consisting of an encoder $F_{enc}(\cdot)$ followed by a decoder $F_{dec}(\cdot)$. The input data from the first-hop passive party is fed into an encoder with three hidden layers to compute the embedding approximations $\hat{E}$. We input these predicted embeddings into the decoder to reconstruct the original input data. The model designs the dimensions of each layer in the encoder and then mirrors these dimensions for the decoder, creating a symmetric structure. Specifically, for the overlapping data $X_{P1|P2}$ with embeddings E, we compute both the embedding loss between the encoder's output and extracted hidden embeddings, and the reconstruction loss between the decoder's output and original overlapped input. For the remaining data $\overline{X_{P1|P2}}$ without embeddings, where $\overline{X_{P1|P2}} = X_{P1} - X_{P1|P2}$, we only compute the reconstruction loss. The total embedding approximation loss is defined as:

$$\mathcal{L}_{app} = \begin{cases} \lambda \mathcal{L}_{emb}(F_{enc}(x), E) + (1-\lambda)\mathcal{L}_{rec}(F_{dec}(F_{enc}(x)), x), & \text{if } x \in X_{P1|P2} \\ \mathcal{L}_{rec}(F_{dec}(F_{enc}(x)), x), & \text{otherwise} \end{cases},$$

where $\lambda \in [0, 1]$ is a hyperparameter to balance the importance between reconstruction and embedding learning. $\mathcal{L}_{emb}(\cdot)$ and $\mathcal{L}_{rec}(\cdot)$ are embedding loss and reconstruction loss, respectively. We set the Mean Squared Error (MSE) for both loss functions. After training, we utilize the trained encoder function $F_{enc}(X_{P1|A}) = \hat{E}$ to obtain embedding approximations $\hat{E}$ for the overlapping data $X_{P1|A}$ from the first-hop passive party in conjunction with the active party.

3.3 Teacher and Student Models

Teacher Model. In our enhanced VFL system, instead of directly using $X_{P1|A}$ to train the local model, we utilize the embedding approximations $\hat{E}$ obtained from $X_{P1|A}$. Both local models and the global model share a three-hidden-layer neural network structure, with dropout used for regularization. The VFL global loss with cross-entropy is defined as:

$$\mathcal{L}_{vfl}(\hat{Y}, Y) = -\sum_{i=1}^{C} Y_i \log(\hat{Y}_i),$$

where $\hat{Y}$ denotes the predicted probability distribution, Y is the one-hot encoded true label, and i indexes the classes. The VFL system acts as the teacher model, generating soft labels $\tilde{Y}$ from $\hat{Y}$, which are used to supervise the student model.

Student Model. We train a student model with the soft labels $\tilde{Y}$ allowing the active party to conduct inference $\hat{Y}^*$ only with local non-overlapping data X_A^*. We implement the student model as a neural network with three hidden layers, where the loss function minimizes the difference between the soft labels

and the local predictions, employing the Kullback-Leibler (KL) divergence [12]. The distillation loss is defined as:

$$\mathcal{L}_{dis}(S(X_A), \tilde{Y}) = D_{KL}(\tilde{Y}||S(X_A)) = \sum_i \tilde{Y}_i \log\left(\frac{\tilde{Y}_i}{S(X_A)_i}\right),$$

where $S(\cdot)$ is the student model.

Algorithm. We introduce the pseudo-algorithm of the main structure (first three modules) in Algorithm 1.

Algorithm 1 VFL-ASP

Input: Overlapping data $X_{P2}, X_{P1|P2}, X_{P1|A}, X_A$
Output: VFL prediction $\hat{Y}$ (soft labels $\tilde{Y}$)
Step 1: Embedding Extraction
for each passive party X_i in $\{X_{P1|P2}, X_{P2}\}$ **do**
    Receive orthogonal matrix P from a trusted third party
    Encrypt data: $X_i^\epsilon \leftarrow PX_i$
    Send X_i^ϵ to the central server (active party)
end for
Central server computes SVD: $X^\epsilon = U^\epsilon \Sigma^\epsilon V^{\epsilon T}$
Each party receives $U^\epsilon \Sigma^\epsilon$ and extracts hidden embeddings: $E \leftarrow [P^T U^\epsilon]\Sigma^\epsilon$
Step 2: Embedding Approximation
Train autoencoder on passive party data X_{P1}:
Obtain embedding loss: $\mathcal{L}_{emb}$ with encoder $F_{enc}(\cdot)$
Obtain reconstruction loss: $\mathcal{L}_{rec}$ with decoder $F_{dec}(\cdot)$
Minimize total loss:

$$\mathcal{L}_{app} \leftarrow \begin{cases} \lambda \times \mathcal{L}_{emb} + (1-\lambda) \times \mathcal{L}_{rec}, & \textbf{if } x \in X_{P1|P2} \\ \mathcal{L}_{rec}, & \textbf{otherwise} \end{cases}$$

Approximate embeddings: $\hat{E} \leftarrow F_{enc}(X_{P1|A})$
Step 3: VFL Model
for each local party $\hat{E}, X_A$ **do**
    Train local model M_i
    Send intermediate result H_i to global model G
    Receive gradients to update parameters θ_i
end for
Combine local outputs to train global VFL model G
Minimize global loss: $\mathcal{L}_{vfl}(\hat{Y}, Y)$
Update global parameter ϕ and send gradients back to local
Repeat above process until convergence criterion is met
return predictions $\hat{Y}$ (soft labels $\tilde{Y}$)

4 Experiments

We evaluate VFL-ASP against two baseline methods on three real datasets, testing diverse feature splits and sample overlaps. Additionally, we assess the student model, analyze runtime efficiency, and perform an ablation study showing the effectiveness of our embedding extraction module.

4.1 Experimental Setup

We implement VFL-ASP using PyTorch 1.10, Python 3.8, and use an NVIDIA GeForce RTX 4090, Intel(R) Xeon w5-2455X @ 3.20 GHz. Without loss of generality, we designate a single party to each of the second-hop and first-hop roles. Following a permutation importance analysis for all features to identify the importance score, we manually assign critical features to the second-hop party and measure classification accuracy with a 95% confidence interval across 100 runs.
Datasets. We evaluate VFL-ASP on three real datasets:
Breast Cancer [25]: The Wisconsin Breast Cancer data contains features from digitized images of breast mass aspirates [25]. The data has $\mathbb{R}^{569\times30}$ dimensions with binary diagnosis labels (malignancy, benign).
MIMIC-III [11]: The MIMIC-III database covers vital signs, lab tests, and medication from over 40k patients with 58k ICU stays [11]. The data has $\mathbb{R}^{58976\times15}$ dimensions and we use the length of stay (four classes) as the prediction label.
Credit [27]: The dataset describes customer default payments, including credit limit and payment history. The data has $\mathbb{R}^{30000\times23}$ dimensions, with a binary label indicating whether a customer defaults on their credit card payment.
Baselines. We comparatively evaluate the classification accuracy and runtime performance of VFL-ASP against baselines:
VFL-STD [19]: The standard VFL model where each first-hop passive and active party trains a local model using its private data, and sends the intermediate results to the active party for the global model training in each communication round. For simplicity, we use a consistent three-layer neural network structure for the local and global models, varying only in the input and output dimensions.
LOCAL: The active local model that only leverages feature information from the active party to train the model and conduct inference.

The implementation code for VFL-ASP framework is available in the anonymous repository [1].

4.2 Experimental Results

Exp-1: Feature Split. Figure 5 illustrates the comparative accuracy as the feature number split changes across parties. Specifically, the feature number is kept equal between the first-hop and active parties, while the number in the second-hop increases incrementally. We observe that VFL-ASP achieves similar performance to VFL-STD across all datasets, but demonstrates greater overall stability on the Breast Cancer dataset, maintaining accuracy around 93%.

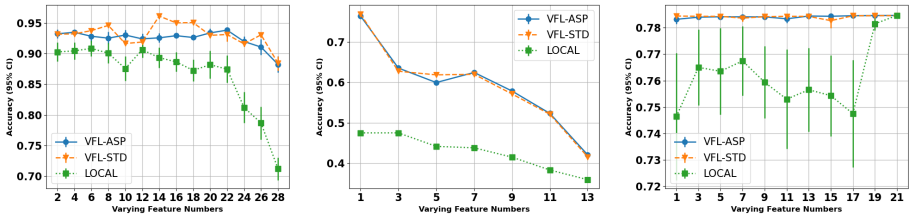

(a) Breast Cancer (b) MIMIC-III (c) Credit

Fig. 5: Comparative accuracy vs. varying feature split.

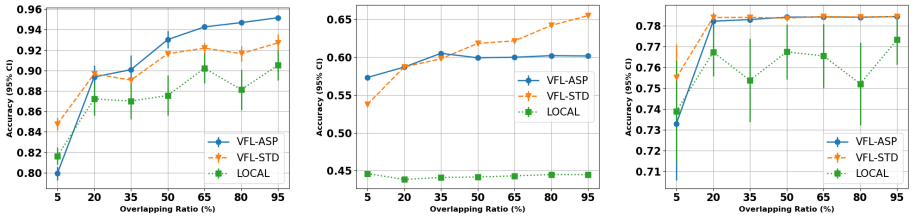

(a) Breast Cancer (b) MIMIC-III (c) Credit

Fig. 6: Comparative accuracy vs. varying sample overlap.

VFL-ASP consistently outperforms the LOCAL model (achieving an average improvement of 5.884%, 16.535%, and 2.238% across three datasets), which shows declining accuracy as the feature increases.

Exp-2: Sample Overlap. We measure the accuracy of VFL-ASP against the baselines for increasing sample overlap between the first-hop and active party, over total overlap with both the active and second-hop parties. We define this overlap ratio as $\alpha = \frac{X_{P1|A}}{X_{P1}}$, where $X_{P1} = X_{P1|P2} + X_{P1|A}$. Figure 6 shows that when $\alpha > 35\%$, VFL-ASP consistently outperforms the baselines on the Breast Cancer dataset as α increases. Compared to VFL-STD, VFL-ASP achieves a comparable accuracy of about 78.5% over the Credit dataset.

Under the general condition with equal feature split and $\alpha = 50\%$ sample overlap across all parties, Table 2 demonstrates that VFL-ASP consistently outperforms the baselines on the Breast Cancer and Credit datasets.

Table 2: Comparative accuracy across models.

Models	Breast Cancer	MIMIC-III	Credit
VFL-ASP	**93.027**±0.840	59.928±0.089	**78.410**±0.028
VFL-STD [19]	91.640±0.243	**61.829**±0.268	78.363±0.132
LOCAL	87.553±1.969	44.160±0.114	76.745±1.313

Exp-3: Student Effectiveness. We compare the student model, supervised via the distilled knowledge from the VFL teacher model, against the local model of the active party. Table 3 highlights that the VFL-ASP student model achieves higher accuracy on the Breast Cancer and MIMIC-III datasets. By leveraging critical features from the second-hop party during inference, it achieves an approximate 3% improvement on the Breast Cancer dataset. In the Credit dataset,

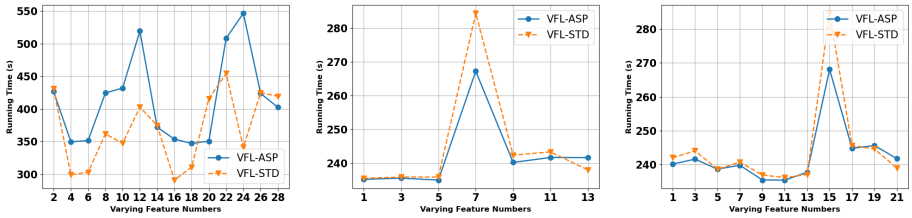

(a) Breast Cancer (b) MIMIC-III (c) Credit

Fig. 7: Comparative runtime performance vs. varying feature split.

VFL-ASP experiences an approximate 1% decrease, likely due to less distinct feature separation and utility between the first-hop and second-hop parties.

Table 3: Student vs. LOCAL accuracy.

Models	Breast Cancer	MIMIC-III	Credit
Student	**89.647**±2.056	**44.869**±0.118	75.511±2.151
LOCAL	86.723±2.410	44.124±0.110	**76.671**±1.321

Exp-4: Runtime Analysis. Figure 7 presents the comparative runtime (total training and inference time) of VFL-ASP versus VFL-STD across three datasets, with varying feature splits among parties. On average, VFL-ASP incurs a 45.137s overhead compared to VFL-STD on the Breast Cancer dataset, but is 2.697s and 1.858s faster on the MIMIC-III and Credit datasets, respectively. The summits in the graphs may result from certain feature splits creating more challenging optimization scenarios, requiring more iterations to achieve comparable accuracy. We implement an early stopping process, which enables VFL-ASP to converge faster than VFL-STD.

Exp-5: Ablation Study. Considering the interdependence between the embedding extraction and approximation modules, we conduct an ablation study to assess the effectiveness of the embedding extraction module. Using a three-layer neural network, we assess four different input configurations as outlined in Table 4. Embedding: extracted embeddings from overlapping data of first and second-hop passive parties. Second-hop/First-hop: raw overlapping data from local passive parties. Centralized: concatenated data from both hops, representing an upper bound for comparison, which is not feasible in an FL system (considered as an ideal case). Table 4 shows that the embeddings achieve the best accuracy on the Breast Cancer and MIMIC-III datasets surpassing the centralized data, and within 0.011% on the Credit dataset. Notably, for all datasets, the embeddings achieve up to 17.063% (first-hop) and approximately 1% (second-hop) accuracy gains, with the greatest improvement shown for the larger MIMIC-III.

Table 4: Ablation study accuracy.

Input Data	Breast Cancer	MIMIC-III	Credit
Embedding: E	**93.400**±0.830	**83.502**±0.112	76.990±0.192
Second-hop data: X_{P2}	92.633±1.040	82.678±0.139	76.941±0.218
First-hop data: $X_{P1\|P2}$	91.033±0.924	66.439±0.238	76.843±0.162
Centralized data: $[X_{P2}, X_{P1\|P2}]$	92.500±1.057	83.472±0.155	**77.001**±0.168

5 Related Work

Recent works have proposed methods to leverage overlapping data between passive and active parties with varying assumptions. For instance, VFedTrans [10] utilizes FedSVD [2] or VFedPCA [3] to extract latent representations of overlapping samples. It employs autoencoder-based methods [7,9] or GANs [6] to transfer knowledge and enrich the local data at the active party. However, VFedTrans only considers one passive and one active party at a time, making it inefficient for multiple passive parties. It also requires overlapping data between the active and passive parties.

VFL-infer [23] leverages knowledge distillation [8] with privileged information to supervise a local student model at the active party with both ground truth and soft labels. However, it assumes direct overlap between the active and all passive parties, limiting its applicability where a subset of passive parties does not directly overlap with the active party.

Lastly, FTL [5, 18, 24] combines (vertical) federated learning and transfer learning [22] to facilitate knowledge sharing across domains while addressing privacy concerns. It projects features into a shared subspace for transfer. However, it is limited to data configurations involving direct data overlap between a single source-domain party and target-domain. VFL-ASP aims to allow transfer without such direct overlap. In general, none of these methods can be directly applied to the data configuration as second-hop overlapping scenarios.

6 Conclusion

We study the VFL problem where the second-hop passive parties do not directly overlap with the active party but share data overlaps with the first-hop parties. This scenario may occur in practice due to restrictive data-sharing constraints. We propose a new model VFL-ASP that incorporates features from second-hop parties into VFL model training. The framework extracts hidden embeddings to capture these features and uses knowledge distillation to conduct inference on the active local party. Our evaluation shows promising accuracy with diverse feature splits and sample overlaps among parties. Through the ablation study, we demonstrate the effectiveness of the embedding extraction module. As the next step, we intend to study client selection strategies that consider data utility and quality in multi-party settings.

References

1. Anonymous: Vertical federated learning across second-hop parties (extended report) (2024), `https://anonymous.4open.science/r/VFL-ASP-B32B`
2. Chai, D., Wang, L., Zhang, J., Yang, L., Cai, S., Chen, K., Yang, Q.: Practical lossless federated singular vector decomposition over billion-scale data. In: Proceedings of the 28th ACM SIGKDD Conference on Knowledge Discovery and Data Mining. pp. 46–55 (2022)

3. Cheung, Y.m., Jiang, J., Yu, F., Lou, J.: Vertical federated principal component analysis and its kernel extension on feature-wise distributed data. arXiv preprint arXiv:2203.01752 (2022)
4. Dang, T.K., Lan, X., Weng, J., Feng, M.: Federated learning for electronic health records. ACM Transactions on Intelligent Systems and Technology (TIST) (2022)
5. Feng, S., Li, B., Yu, H., Liu, Y., Yang, Q.: Semi-supervised federated heterogeneous transfer learning. Knowledge-Based Systems **252**, 109384 (2022)
6. Goodfellow, I., Pouget-Abadie, J., Mirza, M., Xu, B., Warde-Farley, D., Ozair, S., Courville, A., Bengio, Y.: Generative adversarial networks. Communications of the ACM **63**(11), 139–144 (2020)
7. Higgins, I., Matthey, L., Pal, A., Burgess, C.P., Glorot, X., Botvinick, M.M., Mohamed, S., Lerchner, A.: Beta-vae: Learning basic visual concepts with a constrained variational framework. ICLR (Poster) **3** (2017)
8. Hinton, G., Vinyals, O., Dean, J.: Distilling the knowledge in a neural network. arXiv preprint arXiv:1503.02531 (2015)
9. Hinton, G.E., Salakhutdinov, R.R.: Reducing the dimensionality of data with neural networks. Science **313**(5786), 504–507 (2006)
10. Huang, C.j., Wang, L., Han, X.: Vertical federated knowledge transfer via representation distillation for healthcare collaboration networks. In: Proceedings of the ACM Web Conference 2023. pp. 4188–4199 (2023)
11. Johnson, A.E.W., Pollard, T.J., Shen, L., Lehman, L.W.H., Feng, M., Ghassemi, M., Moody, B., Szolovits, P., Anthony Celi, L., Mark, R.G.: Mimic-iii: A freely accessible critical care database. Scientific Data **3**(1), 1–9 (2016)
12. Joyce, J.M.: Kullback-leibler divergence. In: International Encyclopedia of Statistical Science, pp. 720–722. Springer (2011)
13. Kairouz, P., McMahan, H.B., Avent, B., Bellet, A., Bennis, M., Bhagoji, A.N., Bonawitz, K., Charles, Z., Cormode, G., Cummings, R., et al.: Advances and open problems in federated learning. Foundations and Trends® in Machine Learning **14**(1–2), 1–210 (2021)
14. Konečnỳ, J.: Federated learning: Strategies for improving communication efficiency. arXiv preprint arXiv:1610.05492 (2016)
15. Konečnỳ, J., McMahan, B., Ramage, D.: Federated optimization: Distributed optimization beyond the datacenter. arXiv preprint arXiv:1511.03575 (2015)
16. Li, W., Xia, Q., Cheng, H., Xue, K., Xia, S.T.: Vertical semi-federated learning for efficient online advertising. arXiv preprint arXiv:2209.15635 (2022)
17. Lim, W.Y.B., Luong, N.C., Hoang, D.T., Jiao, Y., Liang, Y.C., Yang, Q., Niyato, D., Miao, C.: Federated learning in mobile edge networks: A comprehensive survey. IEEE Communications Surveys & Tutorials **22**(3), 2031–2063 (2020)
18. Liu, Y., Kang, Y., Xing, C., Chen, T., Yang, Q.: A secure federated transfer learning framework. IEEE Intelligent Systems **35**(4), 70–82 (2020)
19. Liu, Y., Kang, Y., Zou, T., Pu, Y., He, Y., Ye, X., Ouyang, Y., Zhang, Y.Q., Yang, Q.: Vertical federated learning: Concepts, advances, and challenges (2023)
20. Liu, Y., Zhang, X., Kang, Y., Li, L., Chen, T., Hong, M., Yang, Q.: Fedbcd: A communication-efficient collaborative learning framework for distributed features. IEEE Transactions on Signal Processing **70**, 4277–4290 (2022)
21. McMahan, B., Moore, E., Ramage, D., Hampson, S., y Arcas, B.A.: Communication-efficient learning of deep networks from decentralized data. In: Artificial Intelligence and Statistics. pp. 1273–1282. PMLR (2017)
22. Pan, S.J., Yang, Q.: A survey on transfer learning. IEEE Transactions on Knowledge and Data Engineering **22**(10), 1345–1359 (2009)

23. Ren, Z., Yang, L., Chen, K.: Improving availability of vertical federated learning: Relaxing inference on non-overlapping data. ACM Transactions on Intelligent Systems and Technology (TIST) **13**(4), 1–20 (2022)
24. Sharma, S., Xing, C., Liu, Y., Kang, Y.: Secure and efficient federated transfer learning. In: 2019 IEEE International Conference on Big Data (Big Data). pp. 2569–2576. IEEE (2019)
25. Wolberg, W., Mangasarian, O., Street, N., Street, W.: Breast cancer wisconsin (diagnostic). UCI Machine Learning Repository (1995), DOI: https://doi.org/10.24432/C5DW2B
26. Yang, Q., Liu, Y., Chen, T., Tong, Y.: Federated machine learning: Concept and applications. ACM Transactions on Intelligent Systems and Technology (TIST) **10**(2), 1–19 (2019)
27. Yeh, I.C.: Default of credit card clients. UCI Machine Learning Repository (2016), DOI: https://doi.org/10.24432/C55S3H
28. Yin, X., Zhu, Y., Hu, J.: A comprehensive survey of privacy-preserving federated learning: A taxonomy, review, and future directions. ACM Computing Surveys (CSUR) **54**(6), 1–36 (2021)